Modeling Falloff Tests in Multilayer Reservoirs

Renan Vieira Bela[a,*], Sinesio Pesco[a], Abelardo Barreto Jr.[a]

[a] *PUC-Rio, Departamento de Matemática*

Abstract

Parameter determination during an injectivity test relies on analytical models that fully foresee how pressure behaves when water is injected in the reservoir. Existing analytical models are able to depict both injection and falloff periods in single-layer reservoirs, but lack to describe the falloff period in multilayer systems. Therefore, this work attempts to extend the existing single-layer falloff formulation to multilayer reservoirs. The accuracy of the proposed solution was assessed by comparison with a numerical simulator. The suggested model was also used to determine the reservoir equivalent permeability.

Keywords: Injectivity Tests, Analytical Modeling, Falloff Period, Commingled Systems

1. Introduction

The injectivity test is a procedure used to collect information over a petroleum reservoir by injecting water into the reservoir. Several reservoir features, such as equivalent permeability and outer boundary condition, might be inferred from the pressure response measured during the test.

Injectivity test consists of two different stages: the injection period and the falloff period. During the former, occurs the water injection into the rock formation. The latter stage is marked by the well shut-in and, hence, a zero-flow pulse propagates along the reservoir.

Over the past years, accomplishments have been made regarding the pressure behavior in multilayer reservoirs under single-phase flow and injectivity tests in single-layer reservoirs. However, an analytical solution for pressure behavior in multilayer reservoirs is well known just during the injection period.

Therefore, this work attempts to develop a new analytical model for the falloff period in multilayer reservoirs. The suggested formulation was reached by combining the solution for injection period in multilayer reservoirs with the existing model for falloff period in single-layer reservoirs. The developed formulation was, then, applied to estimate the reservoir equivalent permeability from pressure data.

2. Previous Achievements

Historically, pressure behavior in petroleum reservoirs has been modeled under two distinct lines of work. On one hand, analytical models for pressure response in multilayer reservoirs under single-phase flow have been developed. In parallel, the study on injectivity tests in single-layer reservoirs has been conducted.

2.1. Modeling Single-Phase Flow in Multilayer Reservoirs

Single-phase flow in multilayer reservoirs has been studied in the context of production tests. However, the same equations also describe a theoretical injectivity test where the reservoir existing oil and the injected fluid present the same properties.

Lefkovits et al. [1] provided an analytical model for production tests in commingled systems. Their model, which has been served as basis for many studies further developed, considers that layer properties may be different in each layer.

Cobb et al. [2] conducted a comparison between three techniques for buildup data analysis in multilayer commingled reservoirs with equal layer thickness: Muskat, Horner and

*I am corresponding author

Email addresses: renanvb1@aluno.puc-rio.br (Renan Vieira Bela), sinesio@puc-rio.br (Sinesio Pesco), abelardo.puc@gmail.com (Abelardo Barreto Jr.)

Miller-Dyes-Hutchinson methods. They have shown that all three mentioned methods might be used to estimate the reservoir flow capacity.

Single-phase flow in multilayer reservoirs with two layers of distinct thickness was studied by Raghavan et al. [3]. A means for obtaining individual layer permeability was proposed, assuming that thickness ratio is known.

Gao [4] developed approximated solutions for pressure and flow-rate in each layer. The suggested formulation is able to provide estimates for flow capacity in each layer.

A procedure for individual layer properties evaluation was reached by Ehlig-Economides and Joseph [5]. The proposed calculation relies on the analysis of pressure and layer flow-rate data.

2.2. Modeling Injectivity Tests in Single-Layer Reservoirs

The study on injectivity tests started to drain greater attention in the 80's. Abbaszadeh and Kamal [6] proposed the waterfront saturation profile depicted by Buckley-Leverett theory [7] may be discretized into a series of banks. Thus, pressure behavior during an injectivity test would be equivalent to the one of a composite reservoir. They also proved that, under certain conditions, waterfront remains stationary during falloff.

Bratvold and Horne [8] evaluated the influence of temperature on fluid mobility and on saturation gradients. Their formulation was also based on discretizing the saturation profile foreseen by Buckley-Leverett theory to compute the pressure response.

A theory for both single-phase and multiphase flow in radially heterogeneous reservoirs was developed by Thompson and Reynolds [9]. They showed that pressure derivative may be understood as a weighted average of the permeabilities along the reservoir. The weighting factor is a function of flow-rate and mobility gradients.

In a subsequent work, Banerjee *et al.* [10] modeled pressure behavior during injectivity tests in radially heterogeneous reservoirs. The same suggested formulation also provides a means for computing the mechanical formation damage in homogeneous reservoirs.

A general theory for the injection period was presented by Peres *et al.* [11]. They showed that their model reduces to the formulation proposed by previous authors, provided that the correct assumptions are made. Their solution is also capable of describing restricted entry wells.

The falloff solution was reached by Peres *et al.* [12], following their own work [11]. The superposition principle was used to describe the flow-rate history during falloff as the sum of two flow-rates with different sign being applied at the same point of the reservoir.

2.3. Modeling Injectivity Tests In Multilayer Reservoirs

The first work regarding injectivity tests in multilayer reservoirs was presented by Barreto *et al.* [13]. They applied Darcy's law to one given layer, so that an expression for the pressure change during the injection period in this layer is obtained. Thereby, layer flow-rate may be written as a function of that individual layer pressure change. Wellbore pressure during injection is, then, computed by summing up all layer flow-rates. Their solution assumes no crossflow and radially infinite reservoir.

As disclosed in this overview, existing analytical models lack to describe falloff period in multilayer systems. Using the formulation reached by Barreto *et al.* [13] as basis, this work will attempt to extend the analytical model for falloff period in single-layer reservoirs [12] to multilayer systems as well. To the author's best knowledge, the developed formulation has not yet been presented before.

3. Reservoir Model

The analytical model developed was based on two fundamental principles: the analytical model for falloff period in single-layer reservoirs [12], and the existing formulation during the injection period in multilayer systems [13]. All calculations assume that a consistent set of units is used and that the reservoir is subject to the following simplifying hypothesis:

- At the instant $t = 0$, reservoir is in equilibrium; *i.e.*, pressure is the same in all layers;
- Homogeneous and isotropic reservoir, with infinite extension;
- Water and oil are assumed to be imiscible, slightly compressible fluids with constant viscosity μ;
- Flow is isothermal;

- Rock formation presents a low and constant compressibility;
- Wellbore fully penetrates all layers and injects at constant flow-rate q_{inj};
- Gravitational and capillary forces are neglected;
- There is no wellbore storage;
- It is considered a commingled system.

Figure 1 displays the considered reservoir model. Reservoir may be composed by an arbitrary number of layers, which may present distinct formation damage zones, or even no formation damage at all. Oil properties, relative permeability curves and rock porosity were assumed to be the same in all layers during the calculations.

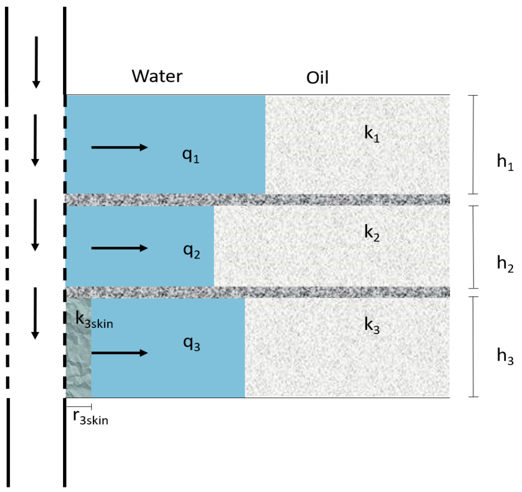

Figure 1: Reservoir Model.

4. Modeling Two-Phase in Multilayer Reservoirs

Darcy's law, which models flow through porous media, is the starting point to compute the pressure variation in the reservoir during an injectivity test [10].

Since the reservoir is composed of multiple layers, Darcy's law is applied in one given layer j [13]. So, considering the reservoir geometry and the model hypothesis, oil and water flow-rates are given by:

$$q_{oj}(r,t) = -\frac{2\pi h_j k_j k_{ro}}{\mu_o}\frac{\partial P_j}{\partial r} \tag{1}$$

and:

$$q_{wj}(r,t) = -\frac{2\pi h_j k_j k_{rw}}{\mu_w}\frac{\partial P_j}{\partial r} \tag{2}$$

Equations (1) and (2) are reached by assuming that relative permeability curves and oil viscosity are the same in all layers. This assumption is made only for a matter of convenience. Both equations can be easily modified if fluid properties are distinct for each layer.

Mass conservation inside the reservoir states that total flow-rate at any layer of a commingled reservoir is computed as:

$$\begin{aligned} q_j(r,t) = q_{wj}(r,t) + q_{oj}(r,t) = \\ -2\pi h_j k_j \left(\frac{k_{ro}}{\mu_o} + \frac{k_{rw}}{\mu_w}\right)\frac{\partial P_j}{\partial r} \end{aligned} \tag{3}$$

At this point, it is convenient to write equation (3) in terms of fluid mobility. This property measures the easiness of one phase to move throughout the porous media. It is defined as the ratio between the phase's relative permeability and its viscosity [9]:

$$\lambda_f(S_w) = \frac{k_{rf}(S_w)}{\mu_f}, \tag{4}$$

Total mobility of the system in study is given by [12]:

$$\lambda_T(S_w) = \lambda_o(S_w) + \lambda_w(S_w) \tag{5}$$

During an injectivity test, a region with high water saturation is formed around the wellbore. As injection goes on, this flooded area grows. Hence, water and oil saturations are functions of time and radius. Then, relative permeabilities and mobilities will also depend on time and radius.

Thereby, Darcy's law may be rearranged, so that pressure change at any point of the reservoir is expressed as a function of the radius:

$$\begin{aligned} -\frac{\partial P_j}{\partial r} &= \frac{q_j(r,t)}{2\pi k_j h_j}\left(\frac{1}{\lambda_o(r,t) + \lambda_w(r,t)}\right)\frac{1}{r} \\ &= \frac{q_j(r,t)}{2\pi k_j h_j}\frac{1}{\lambda_T(r,t)}\frac{1}{r} \end{aligned} \tag{6}$$

Thus, integrating both sides over the radius, from the wellbore onwards [9]:

$$\Delta P_{wf_j}(t) = \frac{1}{2\pi k_j h_j} \int_{r_w}^{\infty} \frac{q_j(r,t)}{\lambda_T(r,t)} \frac{dr}{r} \tag{7}$$

where the wellbore radius is denoted by r_w.

Beyond the waterfront, only oil flows. On the other hand, behind the waterfront, a two-phase flow occurs [6, 8]. Hence, it is logical to split the right side of equation (7) in two integrals, one whose integration limits go from the wellbore to the waterfront and another whose limits go from the waterfront onwards:

$$\Delta P_{wf_j}(t) = \frac{1}{2\pi k_j h_j} \int_{r_w}^{r_{F_j}(t)} \frac{q_j(r,t)}{\lambda_T(r,t)} \frac{dr}{r} + \frac{1}{2\pi k_j h_j} \int_{r_{F_j}(t)}^{\infty} \frac{\hat{q}_{oj}(r,t)}{\hat{\lambda}_o} \frac{dr}{r} \tag{8}$$

In the second integral of equation (8), total flow-rate was replaced by oil flow-rate at irreducible water saturation ($\hat{q}_{oj}$), and total mobility was replaced by the oil mobility at irreducible water saturation ($\hat{\lambda}_{oj}$). This comes from the fact that oil is the only fluid flowing beyond the waterfront [6, 8]. Furthermore, oil and water remain at their respective connate saturations beyond the waterfront, since injected water has not yet reached this region. Thus, oil properties must be evaluated at its endpoint saturation. Waterfront radius, denoted by $r_{F_j}(t)$, is estimated by Buckley-Leverett theory [7].

5. Proposed Formulation

Equation (8) concerns a two-phase flow in a reservoir subject to the assumptions made in section 3. It applies for both injetion and falloff periods. The solution for the injection period was derived from equation (8) by Barreto *et. al* [13].

To reach the formulation for the falloff period, additional assumptions must be made, regarding the physical phenomena that occur after the wellbore is shut.

5.1. Pressure Behavior During Falloff

It is known that the mobility profile remains practically unchanged during falloff [6, 8]. This hypothesis plays an essential role to the computation of wellbore pressure during falloff. If the waterfront were transient, flow-rate throughout the reservoir would also be transient . Pressure behavior, then, could only be solved numerically.

Thus, in equation (8), total mobility profile and waterfront radius depend only on the radius and on the injection time t_p:

$$\Delta P_{ws_j}(\Delta t) = \frac{1}{2\pi k_j h_j} \int_{r_w}^{r_{F_j}(t_p)} \frac{q_{sj}(r,\Delta t)}{\lambda_T(r,t_p)} \frac{dr}{r} + \frac{1}{2\pi k_j h_j} \int_{r_{F_j}(t_p)}^{\infty} \frac{\hat{q}_{osj}(r,\Delta t)}{\hat{\lambda}_o} \frac{dr}{r} \tag{9}$$

where the subscript s denotes the falloff period. Adding and subtracting the term $\frac{1}{2\pi k_j h_j} \int_{r_w}^{r_{F_j}(t_p)} \frac{\hat{q}_{osj}(r,\Delta t)}{\hat{\lambda}_o} \frac{dr}{r}$ in the right side of equation (9):

$$\Delta P_{ws_j}(\Delta t) = \frac{1}{2\pi k_j h_j} \int_{r_w}^{r_{F_j}(t_p)} \left(\frac{q_{sj}(r,\Delta t)}{\lambda_T(r,t_p)} - \frac{\hat{q}_{osj}(r,\Delta t)}{\hat{\lambda}_o} \right) \frac{dr}{r} + \frac{1}{2\pi k_j h_j} \int_{r_w}^{\infty} \frac{\hat{q}_{osj}(r,\Delta t)}{\hat{\lambda}_o} \frac{dr}{r} \tag{10}$$

Equation (10) shows that the pressure variation at the wellbore may be understood as the sum of two terms: one owing to the mobility differences between oil and water ($\Delta P_{\lambda s_j}$), and another related to the single-phase oil flow (ΔP_{os_j}):

$$\Delta P_{ws_j}(\Delta t) = \Delta P_{\lambda s_j}(\Delta t) + \Delta P_{os_j}(\Delta t) \tag{11}$$

where:

$$\Delta P_{\lambda sj}(\Delta t) = \frac{1}{2\pi k_j h_j} \int_{r_w}^{r_{F_j}(t_p)} \left(\frac{q_{sj}}{\lambda_T} - \frac{\hat{q}_{osj}}{\hat{\lambda}_o} \right) \frac{dr}{r} \tag{12}$$

and:

$$\Delta P_{osj}(\Delta t) = \frac{1}{2\pi k_j h_j} \int_{r_w}^{\infty} \frac{\hat{q}_{osj}(r, \Delta t)}{\hat{\lambda}_o} \frac{dr}{r} \quad (13)$$

By hypothesis, there is no formation crossflow and pressure is the same in all layers, apart from the hydrostatic effect. This means that, after the well is shut, the system is in equilibrium and there is no flow between layers, neither through the vertical boundaries between adjacent layers nor through the wellbore. This assumption is not only crucial to the development of the falloff formulation, but also significantly strong.

Assuming that there is no flow between layers means, in other words, to state that vertical flow between layers is so small compared to the horizontal flow along the reservoir, that it may be neglected. This might not be true during falloff if layer properties are remarkably different [14].

From the negligible vertical flow hypothesis, follows that the zero-rate pulse equally propagates along all layers during falloff. Then, total and oil flow-rate may be expressed as functions of layer flow-rate fraction, which is the ratio between the flow-rate in a given layer j evaluated at one given radius and one given instant of time, and the injected flow-rate:

$$q_{D_j}(r, t) = \frac{q_j(r, t)}{q_{inj}} \quad (14)$$

To reach the expression for pressure change during falloff, layer flow-rate fraction within the flooded region is assumed to remain constant after the well is shut, and equal to the flow-rate fraction at $t = t_p$. Then, total and oil flow-rates in layer j may be expressed as:

$$q_{sj}(r, \Delta t) = q_{Dp_j} q_s(r, \Delta t); \quad (15)$$

and:

$$\hat{q}_{osj}(r, \Delta t) = q_{Dp_j} \hat{q}_{os}(r, \Delta t), \quad (16)$$

where q_{Dp_j} is the layer flow-rate fraction just before shut-in, defined as:

$$q_{Dp_j} = \frac{q_j(t = t_p)}{q_{inj}} \quad (17)$$

Thus, equation (10) may be rewritten as:

$$\Delta P_{ws_j}(\Delta t) = \Delta P_{os_j}(\Delta t) + \frac{q_{Dp_j}}{2\pi k_j h_j} \int_{r_w}^{r_{F_j}(t_p)} \left(\frac{q_s}{\lambda_T} - \frac{\hat{q}_{os}}{\hat{\lambda}_o} \right) \frac{dr}{r} \quad (18)$$

It is known that the term $\Delta P_{osj}(t)$ is, in fact, the same for all layers [4, 5, 13]. From now on, this term will be referred to as $\Delta P_{os}(t)$. Furthermore, the considered reservoir model states that pressure change is the same for all layers. So, the pressure measured at the well bottom is equal to the pressure at any individual layer, apart from the hydrostatic effect:

$$\Delta P_{ws_1}(\Delta t) = ... = \Delta P_{ws_n}(\Delta t) = \Delta P_{ws}(\Delta t) \quad (19)$$

Besides, the term multiplying the layer flow-rate fraction will be denoted as a weight variable $R_j(\Delta t)$:

$$R_j(\Delta t) = \frac{1}{2\pi k_j h_j} \int_{r_w}^{r_{F_j}(t_p)} \left(\frac{q_s}{\lambda_T} - \frac{\hat{q}_{os}}{\hat{\lambda}_o} \right) \frac{dr}{r} \quad (20)$$

Thus, an expression to compute q_{Dp_j} is obtained from equation (18):

$$q_{Dp_j} = \frac{\Delta P_{ws}(\Delta t) - \Delta P_{os}(\Delta t)}{R_j(\Delta t)} \quad (21)$$

At any time step, in particular for $t = t_p$, the definition of layer flow-rate fraction ensures that:

$$\sum_{j=1}^{n} q_{D_j} = \frac{1}{q_{inj}} \sum_{j=1}^{n} q_j = 1 \Rightarrow \sum_{j=1}^{n} q_{Dp_j} = 1 \quad (22)$$

Hence, from equations (21) and (22):

$$1 = \sum_{j=1}^{n} \left(\frac{\Delta P_{ws}(\Delta t) - \Delta P_{os}(\Delta t)}{R_j(\Delta t)} \right)$$
$$= (\Delta P_{ws}(\Delta t) - \Delta P_{os}(\Delta t)) \sum_{j=1}^{n} \left(\frac{1}{R_j(\Delta t)} \right) \quad (23)$$

Rearranging equation (23):

$$\Delta P_{ws}(\Delta t) = \Delta P_{os}(\Delta t) + \left(\sum_{j=1}^{n} \frac{1}{R_j(\Delta t)} \right)^{-1} \quad (24)$$

As described in equation (24), pressure change in multilayer reservoirs during falloff may be understood as the sum of the single-phase contribution with one term that encompasses the mobility differences between water and oil, in an analogous way to the injection period.

In single-layer reservoirs, equation (24) reduces to the analytical model for falloff period in single-layer reservoirs proposed by Peres *et al.* [12]. This ensures that the suggested formulation is able to describe pressure behavior during falloff in reservoirs with an arbitrary number of layers.

5.2. Flow-Rate Approximation

The comprehension of the procedure described in section 5.1 shows that an essential step consists of determining flow-rate at any point along the reservoir. Thereby, equation (24) may be applied to compute the pressure change during falloff.

One central question is how to estimate total flow-rate behind the waterfront. Two straightforward and rough approximations come from considering that total flow-rate equals either to oil or to water flow-rate, calculated at their respective endpoint saturations:

$$q_s(r, \Delta t) = \hat{q}_{os}(r, \Delta t) \quad (25)$$

Or:

$$q_s(r, \Delta t) = \hat{q}_{ws}(r, \Delta t) \quad (26)$$

A more accurate approximation is obtained by taking an average between these two flow-rates, weighted by water and oil endpoint saturations:

$$q_s(r, \Delta t) = \frac{\hat{\lambda}_o \hat{q}_{os}(r, \Delta t) + \hat{\lambda}_w \hat{q}_{ws}(r, \Delta t)}{\hat{\lambda}_o + \hat{\lambda}_w} \quad (27)$$

Finally, approximation (27) is improved by accounting for the mobility profile along the flooded area:

$$q_s(r, \Delta t) = \frac{\lambda_o(r) \hat{q}_{os}(r, \Delta t) + \lambda_w(r) \hat{q}_{ws}(r, \Delta t)}{\lambda_o(r) + \lambda_w(r)} \quad (28)$$

An estimation for water and oil flow-rates may be derived from the dimensionless version of Darcy's law:

$$q_D(r, \Delta t) = -r_D \frac{\partial P_D(r, \Delta t)}{\partial r_D}, \quad (29)$$

where q_D, r_D and P_D are the dimensionless flow-rate, radius, and pressure change, defined as:

$$q_D = \frac{q}{q_{inj}}; \quad (30)$$

$$r_D = \frac{r}{r_w}; \quad (31)$$

$$P_D = \frac{kh\hat{\lambda}_f \Delta P}{q_{inj} B_f} \quad (32)$$

The subscript f indicates the flowing phase. Therefore, flow-rate may be easily computed once the pressure change is well defined. For radially infinite flow, a simple and quite accurate estimate for the flow-rate is provided by the source line solution [12]:

$$q_D = exp\left(\frac{-r_D^2}{4t_D} \right) \quad (33)$$

where the dimensionless time t_D is computed as follows:

$$t_D = \frac{\hat{\lambda}_f kt}{\phi c_t r_w^2} \quad (34)$$

At this point, another fundamental assumption is made. In multilayer reservoirs, it was assumed that, if the dimensionless parameters are calculated using the reservoir's total thickness and equivalent permeability, then the source line approximation yields the sum of oil (or water) flow-rate in all layers. Total thickness and equivalent permeability are defined as [1, 2]:

$$h_T = \sum_{j=1}^{n} h_j; \qquad k_{eq} = \frac{1}{h_T} \sum_{j=1}^{n} k_j h_j \quad (35)$$

Definitions for dimensionless radius and flow-rate remain the same as in the single-layer case.

During falloff, pressure change is computed by applying the superposition principle, as depicted by Peres *et al.* [12]:

$$q_{Ds} = exp\left(-\frac{r_D^2}{4t_D} \right) - exp\left(-\frac{r_D^2}{4\Delta t_D} \right) \quad (36)$$

Oil flow-rate at a given radius is evaluated by applying equation (36). Oil properties should be used to compute the dimensionless parameters. On the other hand, water flow-rate is calculated by using water properties to compute the dimensionless variables.

5.3. *Adjustments Due to the Skin Effect*

So far, all calculations assume the reservoir does not present any formation damage. Nevertheless, perforation and completion of the wellbore may create a region with modified permeability (k_{skin}) around it. This phenomena, known as skin effect, results in an additional pressure rise, or drop, depending on the value k_{skin}.

With the purpose of accounting for such effect, the R_j coefficient used in the calculation of ΔP_λ must be adjusted whenever the reservoir presents formation damage. The correction depends on the waterfront position, compared to the skin radius (r_{skin}). While the flooded region is within the damaged zone:

$$R_j(\Delta t) = \frac{1}{2\pi k_{j_{skin}} h_j} \int_{r_w}^{r_{F_j}(t_p)} \left(\frac{q_{sj}}{\lambda_T} - \frac{\hat{q}_{osj}}{\hat{\lambda}_o} \right) \frac{dr}{r} \tag{37}$$

Otherwise, if the waterfront has overcome the damaged zone:

$$R_j(\Delta t) = \frac{1}{2\pi k_j h_j} \left[\int_{r_w}^{r_{F_j}(t_p)} \left(\frac{q_{sj}}{\lambda_T} - \frac{\hat{q}_{osj}}{\hat{\lambda}_o} \right) \frac{dr}{r} + \left(\frac{k_j}{k_{j_{skin}}} - 1 \right) \int_{r_w}^{r_{j_{skin}}} \left(\frac{q_{sj}}{\lambda_T} - \frac{\hat{q}_{osj}}{\hat{\lambda}_o} \right) \frac{dr}{r} \right] \tag{38}$$

6. Results and Discussion

To evaluate the accuracy of the solution proposed in section 5, a set of cases was run on a commercial based flow simulator. Oil model used was *blackoil*.

Pressure variation is expected to change in time as two semilog straight lines, one associated to the oil properties and another governed by the water properties, separated by a transition period [9, 10].

Therefore, in order to properly interpret the results of an injectivity test, one must analyze not only the pressure data, but also the pressure derivative with respect to the logarithm of time (from now on, referred to as pressure derivative). Each semilog straight line is identified by a period when pressure derivative is constant, and reflects the properties of one distinct fluid.

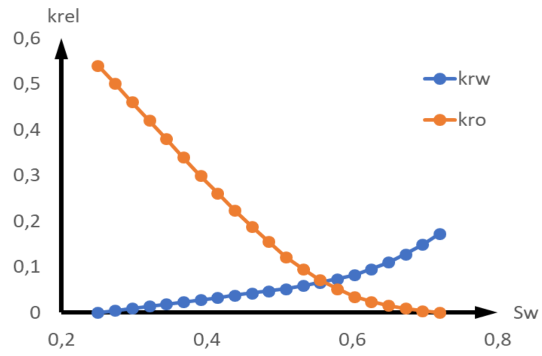

Figure 2: Relative Permeability Curves

6.1. *Input Parameters*

For all cases, it was considered a 4 days (96 hours) injection period followed by a 4 days falloff period, as in a typical injectivity test. The 4 days injection time is short enough so that infinite radial regime is still acting [15]. Injection flow-rate, wellbore radius and other rock and fluid properties may be seen in table 1.

Oil and water relative permeability curves, which were assumed to be the same in every layer, are displayed in figure 2. Water properties were evaluated at a typical reservoir temperature (between 50 and 60 °C).

For all cases, total reservoir thickness was set as 30 m, to ensure that the hypothesis of negligible gravitational effects is valid.

Depending on the relative easiness of water and oil to move through the reservoir, the two-phase flow may be labeled as either favorable or unfavorable to water displacement. One useful parameter to understand which fluid will moves more easily is the endpoint mobility ratio $\hat{M}$:

$$\hat{M} = \frac{\hat{\lambda}_w}{\hat{\lambda}_o} \tag{39}$$

Flows favorable to water displacement imply that $\hat{M} > 1$, while mobility ratios lower than 1 denote the flow is unfavorable to water displacement.

q_{inj} (m^3/d)	r_w (m)	ϕ	c_r ($(kgf/cm^2)^{-1}$)	μ_w (cP)	c_w ($(kgf/cm^2)^{-1}$)	c_o ($(kgf/cm^2)^{-1}$)
500	0.108	0.32	8.0x10^{-5}	0.52	1.14x10^{-4}	4.04x10^{-5}

Table 1: Rock and Fluid Properties

For each reservoir configuration, a pair of values for oil viscosity was chosen such that one would result in a flow favorable to water ($\mu_o = 5.10$ cP) and the other would present a mobility ratio lower than one ($\mu_o = 1.00$ cP). Table 2 shows the reservoir settings for each case.

6.2. Comparison Between Analytical Model and Numerical Simulation

Results for cases depicted in table 2 are displayed in figures 3 to 8. Analytical solution and numerical data showed a good agreement for all cases.

Cases A1 and A2 show the pressure response in a reservoir without formation damage and with different permeabilities in each layer. Thickness is the same in all layers. Difference between individual layer permeabilities is intended to assess whether or not the hypothesis of no flow between layers during falloff is valid.

The pressure behavior in a two-layer reservoir with two distinct damaged regions is displayed in cases B1 and B2. This case aims to evaluate the influence of distinct skin factors in the overall pressure behavior.

Cases C1 and C2 present five distinct layers. Damaged zone properties imply that skin factor is the same in every layer. Again, the hypothesis of negligible flow between layers during falloff is tested.

6.3. Results Analysis and Discussion

It is noticeable that pressure derivative starts at a level during early time and, after a transition period, stabilizes at a different level at long time. This is a typical feature of a two-phase flow.

At early falloff times, pressure is governed by water properties. As the zero-rate pulse reaches the higher oil saturations regions, pressure derivative starts to reflect the properties of this fluid [16]. For cases whose flow is favorable water, the highest pressure derivative level is associated to oil. Similarly, for cases with $\hat{M} < 1$, the highest derivative level is related to water.

Differences between simulated and analytical data are related to the fact that numerical simulation faces convergence issues due to the existence of shocks in the solution [13]. Thus, the transition region between water and oil properties level may be delayed in the numerical simulation.

Early falloff times present some divergences between numerical and analytical data, especially in cases B1 and B2. The main reason for that relies on usage of the source line solution to determine total and oil flow-rates. Such approximation is less accurate in the region closest to the wellbore. As the zero-rate pulse develops, this error becomes less significant.

Moreover, the choice of the total flow-rate approximation is another cause of deviations between numerical and analytical data during early falloff times. Figure 9 compares the

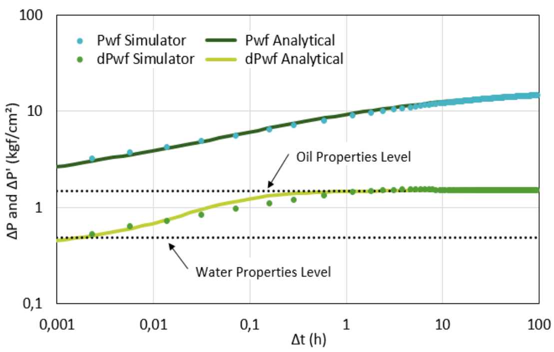

Figure 3: Case A1

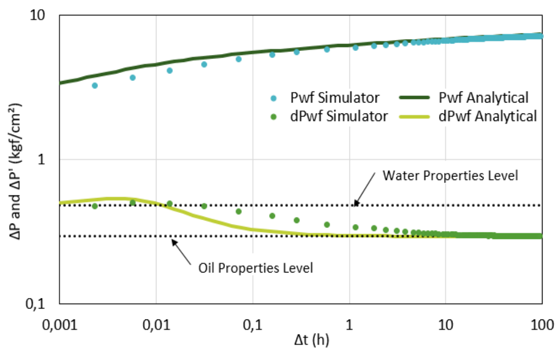

Figure 4: Case A2

Case	Layers	k (mD)	h (m)	k_{skin} (mD)	r_{skin} (m)	$\hat{M}$
A1	3	1500 500 1000	10 (all)	-	-	3.09
A2	3	1500 500 1000	10 (all)	-	-	0.61
B1	2	1000 (all)	15 (all)	500 100	0.5 (all)	3.09
B2	2	1000 (all)	15 (all)	500 100	0.5 (all)	0.61
C1	5	1000 800 1200 900 1400	6 (all)	500 400 600 450 700	0.5 (all)	3.09
C2	5	1000 800 1200 900 1400	6 (all)	500 400 600 450 700	0.5 (all)	0.61

Table 2: Tested Cases

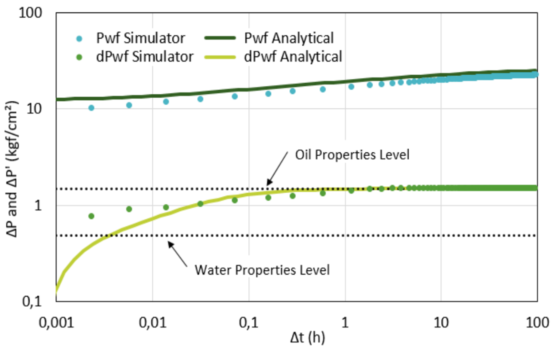

Figure 5: Case B1

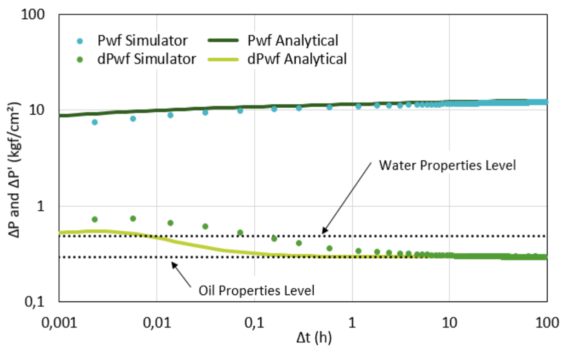

Figure 6: Case B2

results obtained by the analytical model using approximations 1 to 4 (equations (25) to (28)). Reservoir and fluids settings are the same as case A1.

When approximation 1 (equation (25)) is used, the overall derivative behavior is consistent with a two-phase flow. However, approximations 2, 3 and 4 (equations (26) to (28)) yielded a pressure derivative profile incompatible with the physical reality, presenting an oscillatory region before the oil properties level is reached.

Such unexpected fact is possibly related to the development of the formulation for the injection period. The model proposed by Barreto *et al.* [13] is achieved under the hypothesis that the flooded zone is within the steady state region. Hence, inside the waterfront, total flow-rate and oil flow-rate at irreducible water saturation are numerically equal during the injection period. Perhaps the results displayed in figure 9 reflect this assumption, suggesting that, during falloff, total flow-rate should be estimated by the oil flow-rate.

Assuming the reservoir is in hydrostatic equilibrium after shut-in is a quite strong

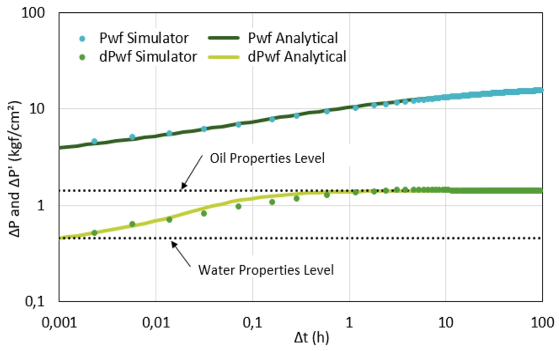

Figure 7: Case C1

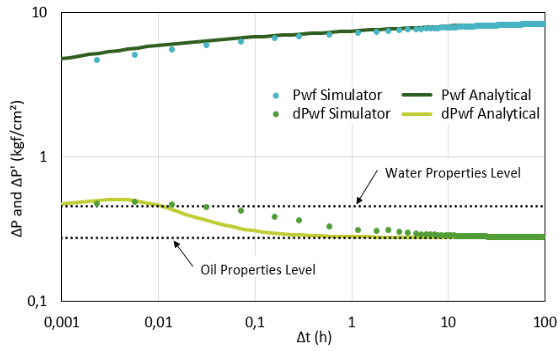

Figure 8: Case C2

hypothesis, specially when layer permeabilities and damaged zones are very different. For these cases, flow between layers through the wellbore may occur right after the well is shut, due to the differences between layer flow capacities [4, 14]. Neglecting this effect is a possible cause of the divergences between analytical and numerical pressure derivatives at early falloff time ($\Delta t < 0.001$ h).

Besides the flow-rate approximation, another possible explanation for this lower derivative level is the accuracy of the Bessel functions used to evaluate ΔP_{os} term. The computation of ΔP_{os} involves modified Bessel functions K_0 and K_1 [13]. For very small time arguments, the imprecision associated to the computational calculation of those functions becomes more relevant.

Thus, initial falloff times are subject to an error that is inherent to the flow-rate approximation and computational issues, but not related to the hypothesis required to reach equation (24). Despite that, as the zero-rate pulse propagates through the reservoir, analytical solution and numerical data rapidly converge, as the zero-pulse propagates throughout the reservoir.

Divergences between analytical solution and numerical simulated data are also related to the numerical calculation procedure. Flow simulator assumes that water is injected by a zero-radius wellbore, that is, well is considered to be a source line. Moreover, the pressure is evaluated as the average pressure in each grid block. This implies the evaluated pressure is influenced by the radial steps in the simulation grid [17]. Although such factors are inherent to the numerical simulation, they are not an issue for the analytical model.

Yet, the errors associated to the flow-rates computation are more relevant in cases with formation damage. The higher flow-rate values estimated by the source line approximation imply in slightly higher values of ΔP_λ when total flow-rate is estimated through equation (25). In cases with $\hat{M} > 1$, the pressure term associated to the mobility differences is negative. Hence, during initial falloff times, this reflects in lower pressure derivative values. In cases whose flow is unfavorable to water, this error is hidden, since the ΔP_λ term is already positive. As the zero-rate pulse propagates throughout the reservoir, this effect gradually vanishes and analytical and simulated data converge.

6.4. Determining the Reservoir Equivalent Permeability

As mentioned in section 6.3, two flatten regions are seen in the pressure derivative profile: one defined by the oil mobility and another related

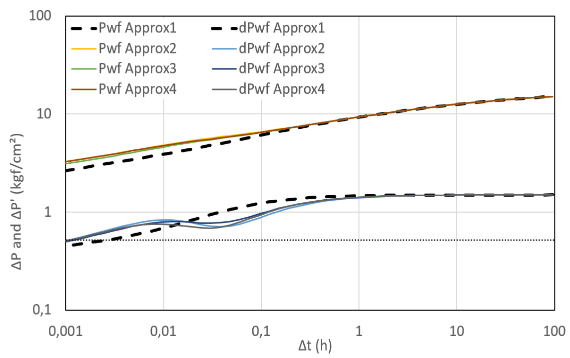

Figure 9: Falloff Data for Case A1 Using Different Flow-Rate Approximations

Case	k_{eq} (mD)	Phase	m_f	k_{eq} Calc. (mD)	Error (%)
A1	1000	Oil	1.483	1010	1.0
		Water	0.508	955	-4.5
A2	1000	Oil	0.295	995	-0.5
		Water	0.522	929	-7.1
B1	1000	Oil	1.486	1008	0.8
		Water	0.351	1382	38.2
B2	1000	Oil	0.295	995	-0.5
		Water	0.536	905	-9.5
C1	1060	Oil	1.399	1070	1.0
		Water	0.505	960	-9.4
C2	1060	Oil	0.278	1056	-0.4
		Water	0.492	986	-7.0

Table 3: Calculated Equivalent Permeabilities

to water properties. Thus, two straight lines are observed in the semilog pressure vs. time graph [9, 10]. Hence, the reservoir equivalent permeability may be estimated using the following equation, derived from the single-phase formulation:

$$k_{eq} = \frac{1.151 \alpha_p q_{inj}}{\overline{h} \hat{\lambda}_f m_f}, \qquad (40)$$

where α_p is a unit conversion constant. For a consistent set of units, $\alpha_p = 1$, whereas for the set of Brazilian field units, $\alpha_p = 19.03$. The straight line angular coefficient is denoted by m_f, where the subscript f indicates the phase associated to the straight line considered.

Therefore, falloff data were used to generate semilog graphs. Pressure data were plotted against Horner time. Results are displayed in table 3.

Equivalent permeability calculated according to equation (40) using semilog graphs were very close to the input values for all cases, both for water and oil properties, expect case B1. Due to the same causes discussed in section 6.3, analytical model is subject to noticeable error during early falloff times (that means, higher Horner times). Hence, the formation of the first semilog straight line may be impaired. Case B1 was more sensitive to those factors, even though they were present in all cases. However, semilog lines associated to oil properties allowed the estimation of equivalent permeabilities with an error smaller than 1% for all cases.

It is interesting to notice that, in field tests, early falloff data usually present too much noise and is subject to storage effect. Thus, water semilog straight line may not be detectable, and the reservoir equivalent permeability is estimated using the straight line relative to oil properties in a typical field test. That means the analytical data allowed an accurate estimate for the equivalent permeability when the most relevant straight line (the one associated to oil mobility) is used.

7. Conclusions

Based on the formulation for falloff period in single-layer reservoirs proposed by Peres *et al.* [12], an expression for multilayer reservoirs was developed. The suggested model is analogous to the injection period solution, formulated by Barreto *et al.* [13].

The proposed model was applied on a set of cases, with distinct number of layers, layer permeabilities and layer skin factors. For all cases, comparison between analytical solution and numerical simulation showed a close agreement.

This indicates that, after the well is shut, vertical flow between layers through the wellbore is negligible, even if layer permeability are different. Such strong hypothesis was essential to reach the analytical model for falloff period in multilayer reservoirs. Results suggest that this fact may not be true in reservoirs with significantly different individual layer skin factors.

Total flow-rate along the reservoir were computed using different approximations. Falloff pressure derivative profiles presented an unexpected result, showing that approximating total flow-rate by the oil flow-rate yields the most realistic pressure

derivative behavior, although this is the roughest way to approximate total flow-rate.

The proposed formulation was also successfully used to estimate the reservoir equivalent permeability using falloff data and oil properties. For all simulated cases, calculated values showed an error smaller than 1%.

Such results verified that the proposed formulation was accurate to describe falloff pressure behavior in multilayer systems.

Nomenclature

B_f = Phase f formation volume factor
c_t = Total compressibility
h_j = Thickness of layer j
k_j = Absolute permeability in layer j
k_{rf} = Relative permeability of phase f
P = Pressure
P_{wf} = Wellbottom hole pressure
q_j = Total flow-rate in layer j
q_{fj} = Flow-rate of phase f in layer j
r = Radius
r_{F_j} = Waterfront radius in layer j
r_w = Wellbore radius
S_w = Water saturation
t = Time
λ_f = Mobility of phase f
$\hat{\lambda}_f$ = Endpoint mobility of phase f
ϕ_j = Porosity in layer j
μ_{fj} = Viscosity of phase f

Acknowledgements

Authors would like to thank Petrobras for the financial support during this work.

References

[1] LEFKOVITS, H.C.; HAZEBROEK, P.; ALLEN, E. E.; MATTHEWS, C. S., A Study of the Behavior of Bounded Reservoirs Composed of Stratified Layers, SPE Journal March (1961) 43–58.

[2] COBB, W. M.; RAMEY JR., H. J.; MILLER, F. G., Well-Test Analysis for Wells Producing Commingled Zones, Journal of Petroleum Technology January (1972) 27–37.

[3] RAGHAVAN, R.; TOPALOGLU, H. N.; COBB, W. M.; RAMEY JR. H. J., Well-Test Analysis for Wells Producing From Two Commingled Zones of Unequal Thickness, Journal of Petroleum Technology September (1974) 1035–1043.

[4] GAO C., Determination of Parameters for Individual Layers in Multilayer Reservoirs by Transient Well Tests, SPE Evaluation Formation March (1987) 43–65.

[5] EHLIG-ECONOMIDES, C. A.; JOSEPH, J., A New Test for Determination of Individual Layer Properties in a Multilayered Reservoir, SPE Evaluation Formation September (1987) 261–283.

[6] ABBASZADEH, M.; KAMAL, M., Pressure-Transient Testing of Water-Injection Wells, SPE Reservoir Engineering February (1989) 115–124.

[7] BUCKLEY, S. E.; LEVERETT, M. C., Mechanism of Fluid Displacement in Sands, Petroleum Technology May (1941) 107–116.

[8] BRATVOLD, R. B.; HORNE, R. N., Analysis of Pressure-Falloff Tests Following Cold-Water Injection, SPE Formation Evaluation September (1990) 293–302.

[9] THOMPSON, L. G.; REYNOLDS, A. C., Well Testing for Radially Heterogeneous Reservoirs Under Single and Multiphase Flow Conditions, SPE Evaluation Formation March (1997) 57–64.

[10] BANERJEE, R.; THOMPSON, L. G.; REYNOLDS, A. C., Injection/Falloff Testing in Heterogeneous Reservoirs, SPE Reservoir Evaluation & Engineering December (1998) 519–527.

[11] PERES, A. M. M.; BOUGHARA, A. A.; CHEN, S.; MACHADO, A. A. V.; REYNOLDS. A. C., Approximate Analytical Solutions for the Pressure Response at a Water Injection Well, SPE Journal September (2004) 1–17.

[12] PERES, A. M. M.; BOUGHARA, A. A.; REYNOLDS, A. C., Rate Superposition for Generating Pressure Falloff Solutions, SPE Journal September (2004) 364–374.

[13] BARRETO JR, A.; PERES, A.; PIRES, A., Water Injectivity Tests on Multilayered Oil Reservoirs, SPE Evaluation Formation 524 (2011) 1–11.

[14] RAGHAVAN, R, Behavior of Wells Completed in Multiple Producing Zones, SPE Evaluation Formation June (1989) 219–230.

[15] SILVA, T. M. D., Modelagem Assistida de Lobos Turbidíticos Baseada em Dados de Teste de Formação, Ms thesis, Pontifícia Universidade Católica do Rio de Janeiro (PUC-Rio), 2017.

[16] CHEN, S.; LI, G.; PERES, A. M. M.; REYNOLDS, A. C., A Well Test for In-Situ Determination of Relative Permeability Curves, SPE Journal October (2005) 1–16.

[17] PEACEMAN, D. W., Interpretation of Well-Block Pressures in Numerical Reservoir Simulation, SPE Journal June (1978) 183–194.